Super-Resolution Imaging

International Edition: DOI: 10.1002/anie.201909220
German Edition: DOI: 10.1002/ange.201909220

Nanographenes: Ultrastable, Switchable, and Bright Probes for Super-Resolution Microscopy

Xiaomin Liu[+], Shih-Ya Chen[+], Qiang Chen, Xuelin Yao, Márton Gelléri, Sandra Ritz, Sachin Kumar, Christoph Cremer, Katharina Landfester, Klaus Müllen, Sapun H. Parekh, Akimitsu Narita, and Mischa Bonn**

Abstract: *Super-resolution fluorescence microscopy has enabled important breakthroughs in biology and materials science. Implementations such as single-molecule localization microscopy (SMLM) and minimal emission fluxes (MINFLUX) microscopy in the localization mode exploit fluorophores that blink, i.e., switch on and off, stochastically. Here, we introduce nanographenes, namely large polycyclic aromatic hydrocarbons that can also be regarded as atomically precise graphene quantum dots, as a new class of fluorophores for super-resolution fluorescence microscopy. Nanographenes exhibit outstanding photophysical properties: intrinsic blinking even in air, excellent fluorescence recovery, and stability over several months. As a proof of concept for super-resolution applications, we use nanographenes in SMLM to generate 3D super-resolution images of silica nanocracks. Our findings open the door for the widespread application of nanographenes in super-resolution fluorescence microscopy.*

Introduction

Super-resolution fluorescence microscopy has enabled visualizing structures with a resolution substantially better than that prescribed by the physics of diffraction-limited conventional microscopy.[1,2] Several important approaches to super-resolution fluorescence microscopy rely on fluorophores switching between bright, emissive (on) and dark (off) states stochastically when they are continuously excited by light. This phenomenon underlies single-molecule localization microscopy (SMLM), for example, stochastic optical reconstruction microscopy (STORM),[3] photoactivated localization microscopy (PALM),[4] and minimal emission fluxes (MINFLUX) microscopy in the localization mode.[5] Presently, four classes of photoswitchable fluorophores are used in such applications: small-molecule organic dyes,[6,7] photoactivatable/switchable fluorescent proteins,[8,9] inorganic quantum dots (QDs),[10–12] and carbon dots (CDs).[13–16] Each class of fluorophores has its strengths and weaknesses from either a photophysical or application perspective.[17] Briefly, organic dyes, such as Alexa 647, the gold standard in SMLM, are small molecules with excellent blinking properties like high photon numbers and low on-off duty cycles. However, their photophysical properties are strongly environmentally (buffer) dependent, restricting their use for super-resolution imaging to specific environments, and the imaging buffer typically has a limited chemical reaction lifetime (less than several hours) after preparation. Photoactivatable/switchable fluorescent proteins have exquisite target molecule specificity but have the issue of low photon numbers resulting in a lower localization precision compared to organic dyes.[18] QDs are very photostable and bright, but their large size ($\approx$10 nm) and high on-off duty cycle[10] limit their function as reliable minimally invasive probes. Also, the toxicity of QDs contain-

[*] Dr. X. Liu[+,++], Q. Chen, X. Yao, Dr. S. Kumar, Prof. Dr. K. Landfester, Prof. Dr. K. Müllen, Prof. Dr. S. H. Parekh, Prof. Dr. A. Narita, Prof. Dr. M. Bonn
Max Planck Institute for Polymer Research
Ackermannweg 10, 55128 Mainz (Germany)
E-mail: liuxiaomin@mpip-mainz.mpg.de
bonn@mpip-mainz.mpg.de
S. Chen[+,++], Dr. M. Gelléri, Dr. S. Ritz, Prof. Dr. C. Cremer
Institute of Molecular Biology gGmbH (IMB)
Mainz (Germany)
Prof. Dr. C. Cremer
Department of Physics, University of Mainz (JGU)
Mainz (Germany)
and
Institute for Pharmacy and Molecular Biotechnology (IPMB)
and Kirchhoff Institute for Physics (KIP)
University of Heidelberg
Heidelberg (Germany)
Prof. Dr. K. Müllen
Institute of Physical Chemistry
Johannes Gutenberg-University Mainz
Mainz (Germany)
Dr. S. Kumar, Prof. Dr. S. H. Parekh
Department of Biomedical Engineering
University of Texas at Austin
Austin, TX (USA)
Prof. Dr. A. Narita
Organic and Carbon Nanomaterials Unit
Okinawa Institute of Science and Technology Graduate University
Okinawa (Japan)
[+] These authors contributed equally to this work.
[++] co-first authors
Supporting information and the ORCID identification number for one of the authors of this article can be found under: https://doi.org/10.1002/anie.201909220.

© 2019 The Authors. Published by Wiley-VCH Verlag GmbH & Co. KGaA. This is an open access article under the terms of the Creative Commons Attribution Non-Commercial License, which permits use, distribution and reproduction in any medium, provided the original work is properly cited, and is not used for commercial purposes.

ing heavy metal atoms may restrict their applicability in biomedicine.[19] CDs have environment-independent blinking properties and are smaller than QDs; however, the undefined/mixed chemical structures not only induce broader fluorescence absorption and emission spectra but also make target-specific binding difficult.

Graphene quantum dots (GQDs) are nanoscale graphene fragments with well-defined, quantized energy levels and have recently been proposed as an environmentally friendly alternative to CDs and QDs.[20] GQDs are, in principle, superior for microscopy imaging due to their small size (typically < 10 nm) and low toxicity. The synthetic approaches to GQDs can be classified in general as top-down or bottom-up approaches. The top-down synthesis method uses physical or chemical techniques to "cleave" graphene[20] or other carbon allotropes such as C_{60} fullerene[21] and double-walled carbon nanotubes.[22] Such methods produce GQDs varying in size and chemical structure, similar to CDs, which results in heterogeneous CD-like photophysical properties. The nanographenes employed in this work are molecularly defined GQDs with a monodisperse character, that is, a precise chemical structure and elemental composition, which are more specifically called (nano)graphene molecules.[23,24] They are obtained by a bottom-up synthesis method which is stepwise derivatization from small organic molecules as starting materials. This method, based on synthetic organic chemistry, not only permits creating nanographenes with well-defined absorption and emission spectra defined by their precise chemical structures, but also enables the introduction of various functional groups[20,25] similarly to organic dyes, e.g., for binding to specific ligands or reactions with specific target molecules. The spectral (absorption and emission) properties of nanographenes can be tailored by engineering the shapes and edge structures with the extension of carbons.[26] These advantages pave the way to develop nanographenes as a new series of fluorophores for optical imaging. While stable fluorescence, i.e., nonblinking emission from nanographenes has been demonstrated,[27–30] this stable, nonblinking, fluorescence has precluded the application of nanographenes from SMLM applications.

Results and Discussion

Here, we demonstrate that, in contrast to previous reports,[27–30] nanographenes show outstanding blinking behavior, combining many of the superior photophysical properties of existing chromophores; they are very small and display blinking independent of the (buffer or air) environment, making them ideal candidates for SMLM. This discovery can be traced to improved nanographene synthesis and better control over the nanographene aggregation behavior. We show that a broad portfolio of nanographenes, for which the chemical structures, and hence absorption and emission spectra, can be precisely tuned, exhibit near-ideal properties as a new class of probes for super-resolution microscopy allowing multiplexing and 3D SMLM.

In this work, we characterize the properties of four types of graphene molecules (**GM**): **DBOV-Mes, GM-C60**, **GM-C78**, and **GM-C96** as blinking probes, benchmarked against Alexa 647, a widely used organic fluorophore in SMLM. These properties include 1) size, 2) absorption and emission spectra, 3) duty cycle (fraction of time a molecule resides in its fluorescent state), and 4) photon number (detected photons per switching event). Figure 1 a,b shows the chemical structures and spectra of **DBOV-Mes**, dibenzo[*hi*,*st*]ovalene (DBOV) with two mesityl (Mes) groups,[31,32] and **GM-C60**[33] with alkyl side chains. **DBOV-Mes (GM-C38)** and **GM-C60** consist of 38 and 60 sp^2-hybridized carbons in their aromatic cores, both with an approximate size of 1 to 2 nm. The chemical structures and spectra of **GM-C78**, **GM-C96**, and Alexa 647 are shown in the Supporting Information, Figures S1 and S2. Table 1 shows general fluorescent characterizations of nanographenes in an organic solvent and Alexa 647 in an aqueous solvent. All of the measured nanographenes exhibit well-defined absorption and emission spectra with different emission wavelengths. In particular, **DBOV-Mes** has very narrow absorption and emission spectra comparable to those of commonly used organic dyes, e.g., Alexa 647, making this nanographene ideal for multicolor imaging.

As mentioned above, Alexa 647 and other organic dyes maintain proper blinking properties in a special blinking buffer. Here we used a standard buffer containing an enzymatic oxygen scavenger system with glucose oxidase and a primary thiol (cysteamine, MEA).[6] Most often due to oxidation reactions or side reactions, these imaging buffers degrade over time, and blinking conditions are maintained only for a few hours.[18] We measured the blinking properties of nanographenes in different environments (i.e., without any blinking buffer) and compared it to Alexa 647 under the optimized conditions (Table 2 and Figures S3–10). As a straightforward measurement to demonstrate the blinking performance of nanographenes in different environments, based on the observation of blinking events, we quantified the duty cycles and the average photon numbers per blinking event for nanographenes in air, in Dulbecco's phosphate-buffered saline (DPBS) buffer, or embedded in a polystyrene (PS) film. As shown by the representative dataset shown in Figure 1 c, nanographene **GM-C60** exhibits intrinsic blinking when exposed to air. Figure 1 d,e shows the duty cycle and the mean photon number per switching event of **GM-C60** as compared to the properties of Alexa 647. Figure 1 f and Table 2 show that **DBOV-Mes** and **GM-C60** in each environment have average photon numbers per blinking event about 1.3-fold higher than those of Alexa 647 in the optimized blinking buffer while maintaining comparable duty cycles and blinking times. This result demonstrates the versatility of nanographene fluorophores compared to small dye molecules; they retain the required properties for SMLM: good blinking in ambient conditions and no special buffer chemistry is needed. Regarding the blinking mechanism of nanographenes, their blinking behavior in different environments indicates a mechanism different from that of traditional organic dyes,[34] semiconductor quantum dots,[35,36] and carbon nanodots.[16,37] Elucidating the blinking mechanism of nanographenes is the topic of ongoing research.

 © 2020 The Authors. Published by Wiley-VCH Verlag GmbH & Co. KGaA, Weinheim

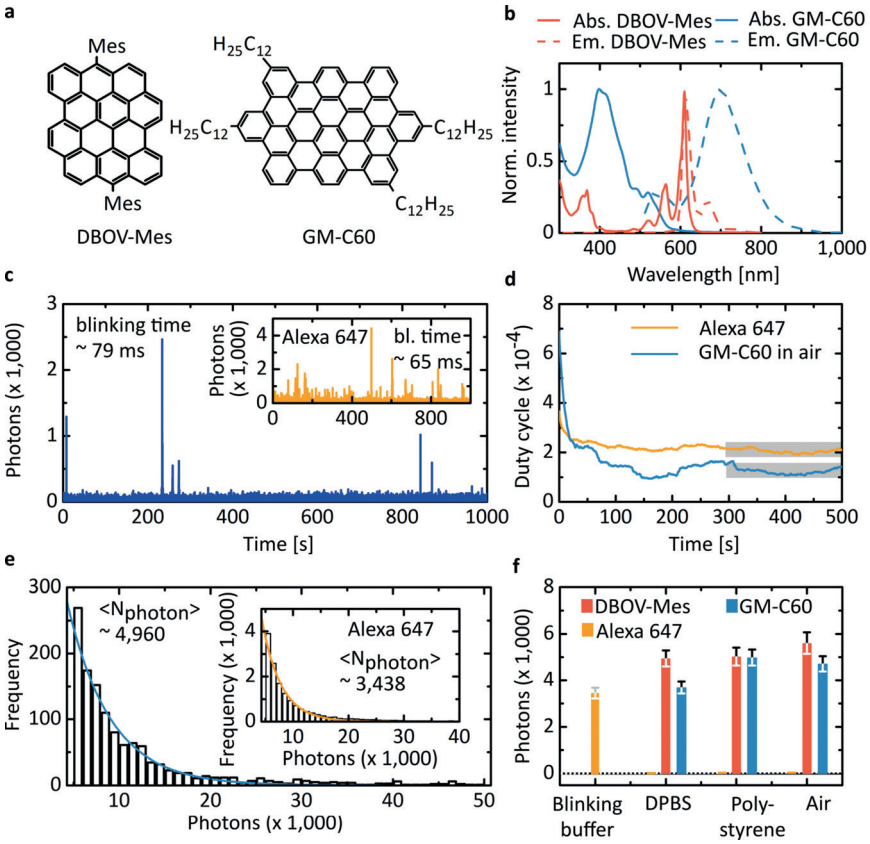

Figure 1. Fluorescence and blinking properties of nanographenes. a) Chemical structures of selected nanographenes, **DBOV-Mes** (**GM-C38**) and **GM-C60**. b) Absorption (solid lines) and emission spectra (dotted lines) of **DBOV-Mes** (red) and **GM-C60** (blue). c) Representative single-molecule fluorescence time trace of **GM-C60** measured in air and of Alexa 647 (inset) in a standard blinking buffer containing thiol (MEA, 10 mM) and an oxygen-scavenging system [(glucose oxidase with catalase (GLOX)]. d) On-off duty cycle (fraction of time a molecule resides in its fluorescent state) of **GM-C60** (blue) and Alexa 647 (orange), calculated from single-molecule fluorescence time traces. The equilibrium duty cycle was calculated within the time window 300–500 s (gray box). e) Histogram of detected photons per switching event and single-exponential fit of **GM-C60** and Alexa 647 (inset). Mean photon numbers were determined by the exponential fit. f) Mean photons detected per switching event for Alexa 647 (orange) in the blinking buffer, **DBOV-Mes** (red) and **GM-C60** (blue) in DPBS, embedded in PS film, and in air, respectively. For Alexa 647, no blinking events could be visualized without the blinking buffer. Error bars are the 95% confidence interval of the fit. Detailed quantitative analysis of Alexa 647 in the blinking buffer, **DBOV-Mes**, and **GM-C60** in different environments and other types of nanographenes embedded in PS film can be found in the Supporting Information, Section 1.

In addition to the excellent blinking properties, we further investigated the photo- and chemical stability of nanographenes **DBOV-Mes** and **GM-C60** by quantifying the photon number per switching event. Figure 2a,b shows the measured mean photons per blinking event of **DBOV-Mes** and **GM-C60** in air and in PS film for freshly prepared samples and samples stored over several months. The blinking properties of both **DBOV-Mes** and **GM-C60** were unchanged over several months. Also, the long-term stability of **DBOV-Mes** was assessed by measuring the absorption spectrum of **DBOV-Mes** dissolved in toluene over six months. We found no changes in the absorption spectrum of the **DOBV-Mes** solution, as shown in Figure S11, indicating low aggregation tendency in organic solvents and high stability of **DBOV-Mes**.

As shown previously,[6,18] the fluorescence emission from some organic dyes, including Alexa 647, can be recovered from a dark (off) state back to the on state with a pulse of ultraviolet or blue light. We performed a similar recovery experiment on nanographenes by first using continuous excitation (532 nm) radiation to send most of the nanographenes to a dark state and then measuring the fraction of molecules that recovered following low irradiance of illumination from a 405 nm laser. Figure 2c shows three raw images from left to right acquired at the beginning of the measurement, after 16 min of continuous illumination with a 532 nm laser, and after a short pulse ($\approx$1.5 s) of 405 nm illumination, respectively. To quantify the fluorescence recovery by 405 nm laser, the number of detected blinking events was analyzed in a time trace of more than 30 min. As shown in Figure 2d, the number of detected blinking events from nanographenes decreased with time over 16 min (20000 frames) from the beginning of the experiment. In the following 15 min, an

Table 1: Fluorescence properties of different nanographenes and Alexa 647 in solution.

Dye	Excitation max. [nm]	Emission max. [nm]	FWHM of excitation spectrum [nm]	FWHM of emission spectrum [nm]	Extinction [$M^{-1}cm^{-1}$]	Quantum yield	Brightness [$M^{-1}cm^{-1}$]
Alexa 647	650[a]	665[a]	38[b]	35[b]	239000[a]	0.33[a]	78870
DBOV-Mes (**GM-C38**)	610	614	15	22	70000	0.79	55300
GM-C60	412	701	84	220	22000	0.1	2200
GM-C78	–[c]	513	–[c]	80	54000	0.02	1080
GM-C96	491	650	83	141	61000	0.01	610

[a] Spectral maxima, extinction coefficient, and quantum yield of Alexa 647 from Ref. [9]. [b] Full width at half maximum (FWHM) of the excitation and emission spectra of Alexa 647 from the dye manufacturer. [c] Peak wavelength and FWHM of **GM-C78** excitation spectrum not available due to the wavelength limitation of the spectrometer. The fluorescence properties of nanographenes were measured in toluene solution.

 © 2020 The Authors. Published by Wiley-VCH Verlag GmbH & Co. KGaA, Weinheim

Table 2: Summary of blinking properties of different nanographenes and Alexa 647.

Dye	Alexa 647	**DBOV-Mes** (GM-C38)			**GM-C60**			**GM-C78**	**GM-C96**
Environment	blinking buffer[a]	DPBS buffer	air	poly-styrene	DPBS buffer	air	poly-styrene	poly-styrene	poly-styrene
Detected photons per switching event	3438	4918	5570	4902	3673	4960	4690	5740	5020
Duty cycle [$\times 10^{-4}$]	2.1	1.3	4.7	8	5.3	1.2	3.2	2.7	1.7
Blinking time [ms]	65	87	108	54	75	79	96	83	94

[a] Blinking properties of Alexa 647 measured in the presence of an enzymatic oxygen-scavenging system [glucose oxidase with catalase (GLOX)] and a primary thiol (MEA, 10 mM). Two representatives of nanographenes, **DBOV-Mes** and **GM-C60**, were measured in three different environments: air, DPBS, and embedded in PS, while the other two nanographenes, **GM-C78** and **GM-C96**, were measured only in a PS film.

additional recovery irradiation (405 nm laser) was administered for 1–2 seconds and was applied on every ≈1000 frames. The number of blinking events clearly shows that a substantial number of nanographenes were switched back into the on state following each 405 nm irradiation. Although both Alexa 647 and **DBOV-Mes** can be transferred into a reversible off state and stochastically activated, the reversible nature of Alexa 647 remains only when it is freshly prepared blinking buffer. On the contrary, the **DBOV-Mes** sample, in air, maintains its blinking behavior even 125 days after preparation, as demonstrated in Figure 2d. From a practical point of view, such reversible activation of the photorecovery property of **DBOV-Mes,** even in air, strongly broadens the potential applications of nanographenes in super-resolution microscopy.

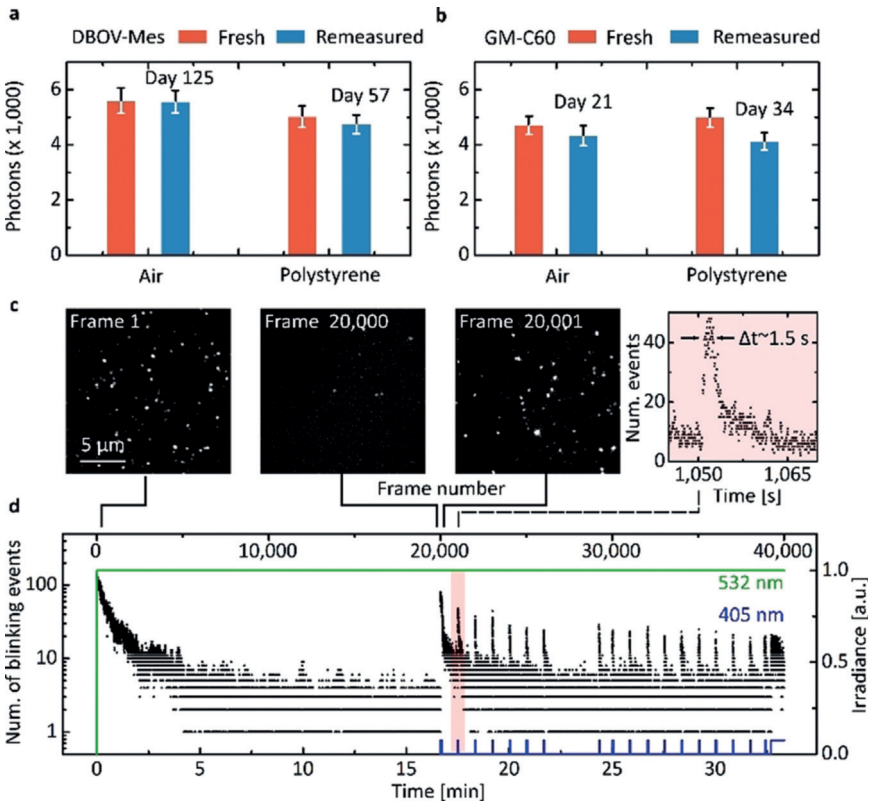

Figure 2. Environmental stability and photorecovery of the nanographenes **DBOV-Mes** and **GM-C60**. a, b) Comparison of the mean number of photons detected per switching event for **DBOV-Mes** and **GM-C60** in air and PS film directly after sample preparation and then remeasured after the waiting time indicated in the legend. Note: The sample of **GM-C60** in air was kept under ambient conditions and not shielded from light before remeasurement. All other samples were stored in a dark environment at room temperature. c) Representative fluorescence images at three selected frames: 1, 20000, and 20001. d) Number of detected blinking events per image frame versus the frame number (time). The first and second images in (c) were acquired more than 16 minutes (20000 frames) apart under continuous 4 kW cm^{-2} excitation with 532 nm (green line). Starting from frame 20001, an additional 405 nm excitation (blue line) with 0.30 kW cm^{-2} was administered for 1–1.65 seconds and this was repeated around every 1000 frames. The number of nanographenes residing in the on state could be repetitively increased by the sample regeneration using the 405 nm excitation. Inset (in pink): an example of fluorescence recovery after exposure to 405 nm laser for around 1.5 seconds. The measured nanographene sample of **DBOV-Mes** in air shown in Figure 2c,d was recorded 125 days after preparation.

As a proof-of-concept for super-resolution microscopy using nanographenes, we prepared nanoscale crevices in glass and imaged them with 3D-SMLM. Afterward, the resulting 3D SMLM image was compared with atomic force microscopy (AFM). Figure 3a shows a schematic of the procedure of depositing nanographenes onto the surface of coverslips and into crevices used for 3D SMLM and AFM imaging. The coverslip was initially examined by conventional brightfield microscopy (Figure S12a) and fluorescence microscopy (Figure S12b). For SMLM, a 2D time series stack of images was acquired, and the raw images were processed to localize nanographenes in 3D within the sample. For 3D localization we first calibrated the microscopy system (Figures S13 and S14), and the **DBOV-Mes** molecules were localized over an axial (z) interval of ±300 nm with an average localization precision of 17.2 nm. A detailed description of the 3D localization and a direct image comparison between conventional microscopy and the 3D SMLM method can be found in the Supporting Information, Section 2. The molecular localizations were sub-

 © 2020 The Authors. Published by Wiley-VCH Verlag GmbH & Co. KGaA, Weinheim

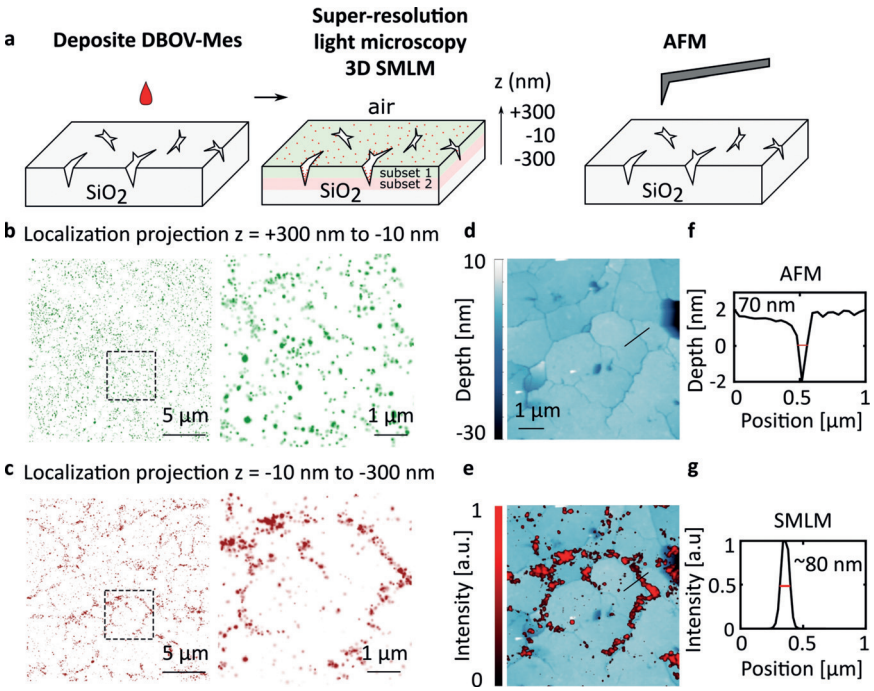

Figure 3. 3D super-resolution microscopy images of nanometer-sized crevices in a glass substrate. a) Imaging procedure for the "etched" coverslips showing crevice features and subsets of molecules localized on (shaded green) or right below (shaded red) the macroscopic (planar) glass surface. After deposition of nanographenes (**DBOV-Mes**) on the coverslips (left), the structure was imaged using 3D SMLM (middle) and AFM (right). The resulting blinking localization of 3D SMLM was classified into two subsets, which indicate the distribution of nanographenes close to (green) and right below (red) the glass–air interface in the cracks. b) For the intensity projection along the *z*-axis between 300 and −10 nm (subset 1) above the "etched" structure, a relatively random spatial distribution of nanographenes was observed. c) For the region between −10 and −300 nm (subset 2), the spatial structure of crevices is apparent. d) AFM reveals the surface structure in the region of interest in (b) and (c). e) Overlay of the SMLM image in (c) and AFM image in (d) shows strong overlapping features after image registration. f, g) Line profiles from AFM (d) and SMLM (c) images show an FWHM about ≈70 nm and ≈80 nm, respectively.

divided into two categories based on the bimodal distribution of localization numbers as a function of axial distance (Figure S14). An intensity projection of the first subset for the z positions from +300 to −10 nm (Figure 3b) shows a relatively homogeneous distribution of nanographenes on the glass surface (not deep into the crevices), as expected. In contrast, the intensity projection from the second subset from $z = -10$ nm to −300 nm (Figure 3c) shows a pattern of nanographenes that is considerably more heterogeneous, as though they are located within the etched, subsurface crevices of the cracks.

As a comparison, AFM was used to scan the substructure of the cracks in the same regions shown in Figure 3b,c. The AFM image reveals a flat surface with numerous cracks (Figure 3d). A larger field of view using the topological scan of AFM in the same region can be found in the Supporting Information, Section 3, Figure S15. After image registration (Figure 3e) of the AFM image and the SMLM image from $z = -10$ nm to −300 nm, the two high-resolution images show highly correlated features at crack locations (Figure 3e), demonstrating that the nanographene localizations in the second subset indeed reveal the substructure of crevices. As shown in the indicated line profiles in Figure 3d,e, the surface profile of the AFM image (Figure 3f) and the intensity profile based on SMLM (Figure 3g) have a similar full width at half maximum (FWHM) of the "crack" of 70 nm and 80 nm, respectively.

Although various techniques have been developed to resolve nanostructures, e.g., X-ray microscopy,[38] AFM,[39] and electron microscopy (EM),[40] these approaches have limitations regarding their applicability. The combination using exceptionally stable and intrinsically blinking nanographenes in 3D SMLM allows visualizing nanostructures in greater depth compared to AFM, where the geometrical restriction of the tip can cause problems, or methods like EM tomography, which requires complete sample destruction.

Conclusion

In summary, nanographenes with atomically defined chemical structures exhibit ideal properties for various super-resolution microscopy methods due to their environmentally independent blinking behavior, large photon numbers, good stability, and well-defined excitation and emission spectra. In our case, the highly pure synthetic production and sample preparation allowed us to discover these properties, which stand in contrast to the general knowledge that nanographenes are constant fluorescent emitters. Atomically precise nanographenes blink in various environments and have high photon numbers per blinking event and low duty cycles in comparison to Alexa 647, the current gold standard small-molecule dye. Moreover, the nanographene dyes exhibit extremely high sample stability of more than 1000-fold longer than Alexa 647. The nanoscale structural imaging of etched cracks in glass demonstrates the potential of nanographenes in super-resolution fluorescence microscopy for applications in materials science. Also, the exquisite chemical control and blinking environment-independent properties of nanographenes offer a great opportunity to investigate blinking mechanisms, which is challenging for organic dyes due to complex buffer dependence and the relatively minimal shelf-life of buffer solutions.[6] Moreover, specific functional side groups can be incorporated at peripheral positions of the nanographenes, for example, hydrophilic groups to enhance the water solubility and binding functionality for protein targeting making nanographenes very promising dyes for bioimaging applications.

 © 2020 The Authors. Published by Wiley-VCH Verlag GmbH & Co. KGaA, Weinheim

Experimental Section

Microscopy

3D SMLM was performed with a SR GSD 3D (Leica) equipped with four lasers: 488 nm (300 mW), 532 nm (500 mW), and 642 nm (500 mW) for excitation, and 405 nm (30 mW) for fluorescence reactivation. An HCX PL APO 160× 1.43 NA Oil CORR-TIRF (Leica) objective and the total internal reflection (TIRF) mode were used for single-molecule blinking measurements and for super-resolution imaging. For all measurements of nanographenes, the 532 nm laser and the emission bandpass filter (550–650 nm/449–451 nm) were used. For the measurements using Alexa 647, the 642 nm laser and the emission bandpass filter (660–760 nm) was used. The microscope was equipped with a back-illuminated EMCCD camera (iXonDU-897, Andor). The resulting images have a pixel size of 100 nm. The detailed description of the setup can be found in the Supporting Information, Section 4.1.

Atomic force microscopy (AFM, Dimension FastScan, Bruker) was done in the tapping mode in air. A standard V-shaped silicon nitride cantilever which has a spring constant of 26 $N m^{-1}$ with a pyramidal tip from Bruker AFM probes (OTESPA-R3) was mounted. The tip has on average a height of 15 μm and a radius of curvature of around 10 nm with a vertex angle of 35° and 18°. Further information about the AFM can be found in the Supporting Information, Section 4.2. AFM images were acquired with a 0.5 Hz line rate, and images with 512 pixels × 512 pixels were acquired.

Experiments for Blinking Properties of Single Nanographenes and Alexa 647

For evaluation of the blinking properties including photon per switching event and on-off duty cycle, nanographene samples were prepared in different embedding media including air, DPBS, and polystyrene. For comparison, additional samples with Alexa 647 were prepared in an oxygen-scavenging system. Detailed information can be found in the Supporting Information, Section 5.

Multiple series of 20000 frames were recorded for every nanographene variant. Nanographenes were excited continuously during imaging with the appropriate wavelength. Images were acquired at an exposure time of 50 ms and an EM gain of 100.

To extract single-molecule time traces, first a maximum intensity projection of the recorded time series was generated. Molecules then were localized in the maximum-intensity projection image, returning the positions of all molecules visible throughout the recorded time series. Single-molecule time traces were then extracted as background-corrected intensities at these positions over all recorded frames. Photon counts and blinking times were determined by localization of single-molecule positions in all frames and merging into blinking events. Resulting histograms of photons per blinking event and blinking duration were fit with a single-exponential function. The reported mean values and errors were extracted from the respective fits. For the detailed description, see the Supporting Information, Section 6.

To investigate the photorecovery characteristics of nanographenes, 40000 frames were acquired with an exposure time of 50 ms and an EM gain of 100. At the first 20000 frames, images were acquired by continuous laser irradiation at 532 nm with an irradiance of 4 $kW cm^{-2}$. While acquiring images from frame 20000 to frame 40000, additionally the 405 nm laser with an intensity of 0.30 $kW cm^{-2}$ was administered for 1–1.65 seconds and this was repeated around every 1000 frames. The images were processed and localizations were determined for analysis.

Experiments for Imaging 3D Crevice Structures

A mild chemical treatment was used to etch nanoscale "cracks" on the surface of a borosilicate coverslip (ibidi, Gridded glass coverslips Grid-50). For fluorescence imaging, 5 μL (1 nM) nanographene in toluene was applied on the coverslip. The detailed sample preparation is described in the Supporting Information, Section 7. For super-resolution imaging of the 3D crevices on the coverslips, the TIRF mode was used to excite the samples with an intensity of 10 $kW cm^{-2}$ at a laser wavelength of 532 nm. 40000 frames with an exposure time of 50 ms and an EM gain of 100 were acquired and processed to determine the 3D localization. AFM images of the same region were acquired, and the resulting image is shown in Figure S15a. The complete overlay image of AFM and SMLM after image registration is shown in Figure S15b for comparison.

Acknowledgements

We acknowledge Max Planck Society and the Human Frontiers in Science Program (RGP0045/2018) for financial support, and the Microscopy Core Facility at IMB for use of the Leica GSD super-resolution microscope. S.-Y.C. acknowledges the international PhD programme on Gene Regulation, Epigenetics & Genome Stability (Mainz, Germany). X.Y. is grateful for the scholarship from China Council Scholarship (CSC). We thank M. Müller and M. Kappl for nanostructure fabrication; L. Driessen for gold film coating on glass; G. Hermann for gold etching; X. Ling for glass cleaning. We thank P. Han, F. Geyer, Y. Yao, and R. Berger for insightful discussions.

Conflict of interest

X. Liu, A. Narita, S. Parekh, Q. Chen, C. Cremer, K. Landfester, K. Müllen, and M. Bonn are listed as inventors on a patent application (application no. 18199451.8 – EPO) and A. Narita, Q. Chen, K. Müllen, X. Liu, S. Parekh, and M. Bonn are listed as inventors on a patent application (application no. 18199447.6 – EPO) related to the work presented in this manuscript. All other authors have nothing to disclose.

Keywords: blinking · chromophores · fluorescence · nanographenes · super-resolution imaging

How to cite: *Angew. Chem. Int. Ed.* **2020**, *59*, 496–502
Angew. Chem. **2020**, *132*, 504–510

[1] L. Schermelleh, A. Ferrand, T. Huser, C. Eggeling, M. Sauer, O. Biehlmaier, G. P. C. Drummen, *Nat. Cell Biol.* **2019**, *21*, 72–84.
[2] S. Pujals, N. Feiner-Gracia, P. Delcanale, I. Voets, L. Albertazzi, *Nat. Rev. Chem.* **2019**, *3*, 68–84.
[3] M. J. Rust, M. Bates, X. Zhuang, *Nat. Methods* **2006**, *3*, 793–796.
[4] E. Betzig, G. H. Patterson, R. Sougrat, O. W. Lindwasser, S. Olenych, J. S. Bonifacino, M. W. Davidson, J. Lippincott-Schwartz, H. F. Hess, *Science* **2006**, *313*, 1642–1645.
[5] F. Balzarotti, Y. Eilers, K. C. Gwosch, A. H. Gynnå, V. Westphal, F. D. Stefani, J. Elf, S. W. Hell, *Science* **2017**, *355*, 606–612.
[6] G. T. Dempsey, J. C. Vaughan, K. H. Chen, M. Bates, X. Zhuang, *Nat. Methods* **2011**, *8*, 1027–1036.
[7] L. Nahidiazar, A. V. Agronskaia, J. Broertjes, B. van den Broek, K. Jalink, *PLoS One* **2016**, *11*, e0158884.
[8] R. M. Dickson, A. B. Cubitt, R. Y. Tsien, W. E. Moerner, *Nature* **1997**, *388*, 355–358.
[9] J. Lippincott-Schwartz, G. H. Patterson, *Trends Cell Biol.* **2009**, *19*, 555–565.
[10] M. Kuno, D. P. Fromm, H. F. Hamann, A. Gallagher, D. J. Nesbitt, *J. Chem. Phys.* **2000**, *112*, 3117–3120.

 © 2020 The Authors. Published by Wiley-VCH Verlag GmbH & Co. KGaA, Weinheim

[11] K. A. Lidke, B. Rieger, T. M. Jovin, R. Heintzmann, *Opt. Express* **2005**, *13*, 7052.
[12] P. Hoyer, T. Staudt, J. Engelhardt, S. W. Hell, *Nano Lett.* **2011**, *11*, 245 – 250.
[13] N. C. Verma, S. Khan, C. K. Nandi, *Methods Appl. Fluoresc.* **2016**, *4*, 044006.
[14] B. Zhi, Y. Cui, S. Wang, B. P. Frank, D. N. Williams, R. P. Brown, E. S. Melby, R. J. Hamers, Z. Rosenzweig, D. H. Fairbrother, et al., *ACS Nano* **2018**, *12*, 5741 – 5752.
[15] H. He, X. Liu, S. Li, X. Wang, Q. Wang, J. Li, J. Wang, H. Ren, B. Ge, S. Wang, et al., *Anal. Chem.* **2017**, *89*, 11831 – 11838.
[16] A. M. Chizhik, S. Stein, M. O. Dekaliuk, C. Battle, W. Li, A. Huss, M. Platen, I. A. T. Schaap, I. Gregor, A. P. Demchenko, et al., *Nano Lett.* **2016**, *16*, 237 – 242.
[17] D. Jin, P. Xi, B. Wang, L. Zhang, J. Enderlein, A. M. van Oijen, *Nat. Methods* **2018**, *15*, 415 – 423.
[18] S. van de Linde, A. Löschberger, T. Klein, M. Heidbreder, S. Wolter, M. Heilemann, M. Sauer, *Nat. Protoc.* **2011**, *6*, 991 – 1009.
[19] U. Resch-Genger, M. Grabolle, S. Cavaliere-Jaricot, R. Nitschke, T. Nann, *Nat. Methods* **2008**, *5*, 763 – 775.
[20] L. Li, G. Wu, G. Yang, J. Peng, J. Zhao, J.-J. Zhu, *Nanoscale* **2013**, *5*, 4015.
[21] G. Chen, Z. Zhuo, K. Ni, N. Y. Kim, Y. Zhao, Z. Chen, B. Xiang, L. Yang, Q. Zhang, Z. Lee, et al., *Small* **2015**, *11*, 5296 – 5304.
[22] F. Li, L. Kou, W. Chen, C. Wu, T. Guo, *NPG Asia Mater.* **2013**, *5*, e60 – e60.
[23] X.-Y. Wang, A. Narita, K. Müllen, *Nat. Rev. Chem.* **2017**, *2*, 0100.
[24] A. Narita, X.-Y. Wang, X. Feng, K. Müllen, *Chem. Soc. Rev.* **2015**, *44*, 6616 – 6643.
[25] Q. Chen, D. Wang, M. Baumgarten, D. Schollmeyer, K. Müllen, A. Narita, *Chem. Asian J.* **2019**, *14*, 1703 – 1707.
[26] Z. Ji, E. Dervishi, S. K. Doorn, M. Sykora, *J. Phys. Chem. Lett.* **2019**, *10*, 953 – 959.
[27] M. Thakur, A. Mewada, S. Pandey, M. Bhori, K. Singh, M. Sharon, M. Sharon, *Mater. Sci. Eng. C* **2016**, *67*, 468 – 477.
[28] X. T. Zheng, A. Ananthanarayanan, K. Q. Luo, P. Chen, *Small* **2015**, *11*, 1620 – 1636.
[29] H. Sun, L. Wu, W. Wei, X. Qu, *Mater. Today* **2013**, *16*, 433 – 442.
[30] S. Zhao, J. Lavie, L. Rondin, L. Orcin-Chaix, C. Diederichs, P. Roussignol, Y. Chassagneux, C. Voisin, K. Müllen, A. Narita, et al., *Nat. Commun.* **2018**, *9*, 3470.
[31] G. M. Paternò, Q. Chen, X.-Y. Wang, J. Liu, S. G. Motti, A. Petrozza, X. Feng, G. Lanzani, K. Müllen, A. Narita, et al., *Angew. Chem. Int. Ed.* **2017**, *56*, 6753 – 6757; *Angew. Chem.* **2017**, *129*, 6857 – 6861.
[32] D. M. Coles, Q. Chen, L. C. Flatten, J. M. Smith, K. Müllen, A. Narita, D. G. Lidzey, *Nano Lett.* **2017**, *17*, 5521 – 5525.
[33] V. S. Iyer, K. Yoshimura, V. Enkelmann, R. Epsch, J. P. Rabe, K. Müllen, *Angew. Chem. Int. Ed.* **1998**, *37*, 2696 – 2699; *Angew. Chem.* **1998**, *110*, 2843 – 2846.
[34] J. Vogelsang, C. Steinhauer, C. Forthmann, I. H. Stein, B. Person-Skegro, T. Cordes, P. Tinnefeld, *ChemPhysChem* **2010**, *11*, 2475 – 2490.
[35] M. Nirmal, B. O. Dabbousi, M. G. Bawendi, J. J. Macklin, J. K. Trautman, T. D. Harris, L. E. Brus, *Nature* **1996**, *383*, 802 – 804.
[36] C. Galland, Y. Ghosh, A. Steinbrück, M. Sykora, J. A. Hollingsworth, V. I. Klimov, H. Htoon, *Nature* **2011**, *479*, 203 – 207.
[37] S. Khan, W. Li, N. Karedla, J. Thiart, I. Gregor, A. M. Chizhik, J. Enderlein, C. K. Nandi, A. I. Chizhik, *J. Phys. Chem. Lett.* **2017**, *8*, 5751 – 5757.
[38] A. Sakdinawat, D. Attwood, *Nat. Photonics* **2010**, *4*, 840 – 848.
[39] F. J. Giessibl, *Rev. Mod. Phys.* **2003**, *75*, 949 – 983.
[40] D. B. Williams, C. B. Carter, *Transmission Electron Microscopy*, Springer US, Boston, **1996**, pp. 3 – 17.

Manuscript received: July 24, 2019
Accepted manuscript online: October 28, 2019
Version of record online: November 26, 2019

 © 2020 The Authors. Published by Wiley-VCH Verlag GmbH & Co. KGaA, Weinheim